

Finally, the radar comprises transmitting and receiving antennas and a high pass amplifier to optimize the data acquisition (DAQ) operation. A PC controls both the ramp generation and the signal acquisition by using the Analog Devices ADF4158 software and LabVIEW, respectively.

2.1. Antenna design

Fig. 2 shows a scheme of the radar on the white cane together with the position of possible obstacles.

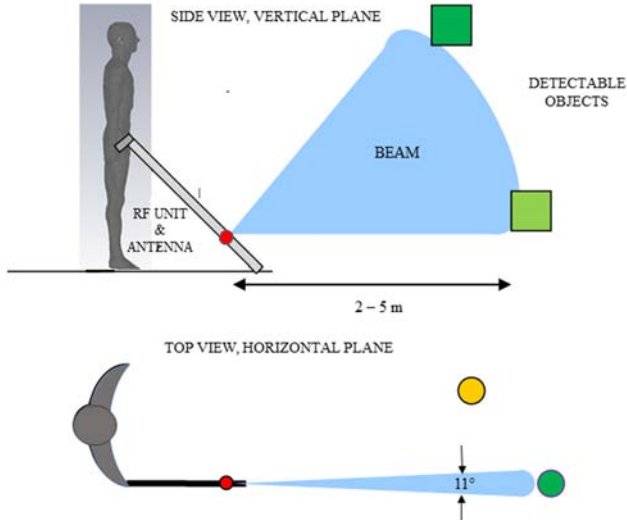


Fig. 2. Scheme of the considered scenario.

A serial patch array has been chosen both for the transmitting and receiving antennas. To design the array the Microwave Studio software by CST has been used. In order to guarantee a field of view between two and five meters, with an azimuthal resolution of about 10° , a 8 patches serial array was necessary. In particular, since the radar output (TX) is differential, a balanced antenna has been realised (see Fig. 3a). Fig. 3b shows the simulated reflection coefficient and Fig. 3c the simulated radiation diagram on the x-z plane for this antenna. Fig. 3b shows the good matching of the antenna in the ISM band while from Fig. 3c a -3 dB aperture of about 10° can be extrapolated together with a maximum gain of about 14 dBi. Concerning the receiving antenna (not shown), it uses the same array in Fig. 3a attached to a Wilkinson power combiner whose two outputs have a phase difference of 180° with each other.

2.2. Power budget

By using the radar equation the received power can be expressed as:

$$P_R = \frac{P_T G_T G_R \sigma \lambda^2}{(4\pi)^3 R^4} \quad (1)$$

where P_T is the transmitted power, G_T and G_R are the transmitting and receiving antenna gains, σ is the target radar cross-section, λ the signal wavelength, and R the target-sensor distance. With $\sigma = 1 \text{ m}^2$ (typical value for a standing subject), $R = 5 \text{ m}$, and $G_T = G_R = 14 \text{ dBi}$ a received power of 1.2 nW is achieved. Since the total voltage gain of the LNA and I&Q demodulator is about 5, an RMS voltage of 1.2 mV is achieved at the in phase output (I). In order to amplify the demodulated signal and filter the 50 Hz noise a 40 dB high pass amplifier ($f_c = 200 \text{ Hz}$) has been added (AMP in Fig. 1).

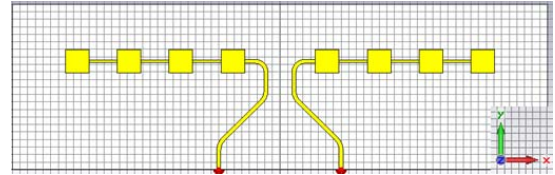
2.3 Radar characteristics

From the FMCW radar theory [12] the range information is converted in output signal frequency through the equation:

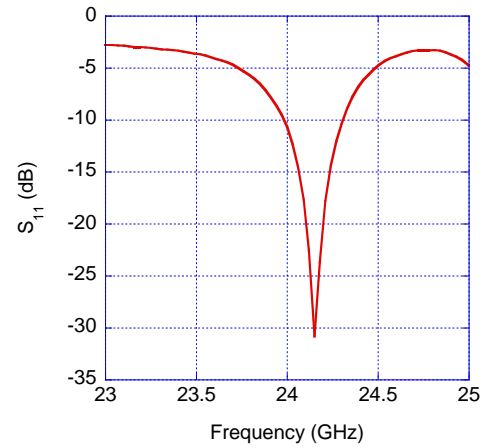
$$f_{Delay} = \frac{2R}{c} \frac{\Delta f}{T} \quad (2)$$

where c is the speed of light, $\Delta f = 250 \text{ MHz}$ is the radar bandwidth and T is the repetition period. Moreover the radar distance resolution is:

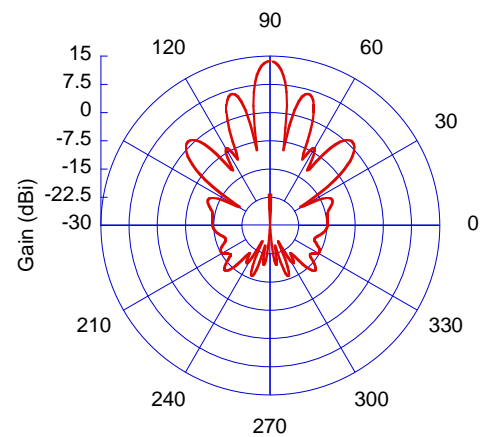
$$\Delta R = \frac{c}{2\Delta f} \quad (3)$$



(a)



(b)



(c)

Fig. 3. (a) Layout of the designed transmitting patch antenna, (b) return loss of the antenna as a function of frequency and (c) antenna simulated gain.

3. RESULTS

The ADF4158 has been programmed to generate a frequency ramp between 1500 MHz and 1515,625 MHz. The ramp is repeated with a frequency of 250 Hz. This frequency ramp at the PLL input port is compared with the VCO output scaled by the factor $R \times N$ and converted in a voltage ramp at the fine input of the VCO.

Fig. 4 shows the assembled radar system with the BGT24MTR11 integrated circuit by Infineon with its serial peripheral interface (SPI) and the AD UG-123 IC. In the figure the realised high pass amplifier is also shown.

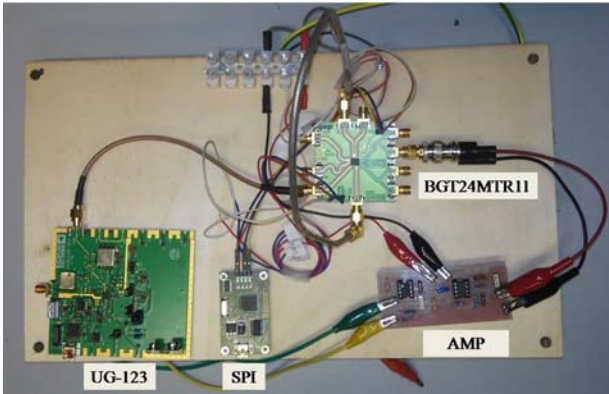


Fig. 4. Picture of the realised prototype.

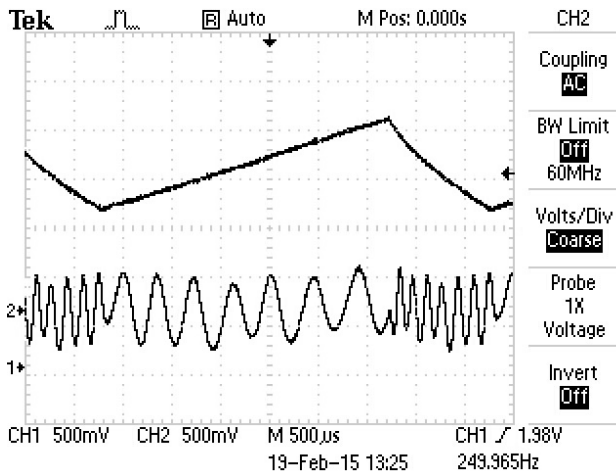


Fig. 5. Voltage ramp at the PLL output together with the output sinusoidal signal.

A first test of the system was conducted placing a 4.5-m long coaxial cable between the input (RFIN) and the output (TX) of the radar. Taking into account the permittivity of the Teflon insulator ($\epsilon_R = 2$) and the round trip delay, this physical length (L) corresponds to an equivalent obstacle distance: $R_{EQ} = L \sqrt{\epsilon_R} / 2 = 3.2$ m. Fig. 5 (upper part) shows the voltage ramp at the fine input of the VCO with a duration of 3 ms together with the voltage at the output (see I in Fig.1). The output sinusoidal signal is clearly visible. In order to measure the output frequency the FFT option of the oscilloscope has been used obtaining a value of 1.74 kHz. By using (2) with $T = 3$ ms, $f_{Delay} = 1.74$ kHz, and $\Delta f = 250$ MHz the measured obstacle range (R_{MEAS}) is equal to 3.13 m, in optimum agreement with the theoretical 3.2 m value.

3.1. Radar characterization

In order to experimentally evaluate the measurement uncertainty of the whole radar system a study has been performed by inserting 9 cables with different lengths between the RFIN and TX radar ports.

Fig. 6 shows the measured distance (R_{MEAS}) as a function of the equivalent obstacle distance (R_{EQ}). On the same figure the ideal radar characteristic $R_{MEAS} = R_{EQ}$ has been reported. In order to better highlight the measurement uncertainty, Fig. 7 shows the differences between measured and equivalent obstacle distance as a function of the equivalent distance itself. The figure highlights a measurement bias of about 0.2 m with a worst case uncertainty of 0.5 m. This value is comparable to the theoretical resolution of 0.6 m calculated from the FMCW signal band.

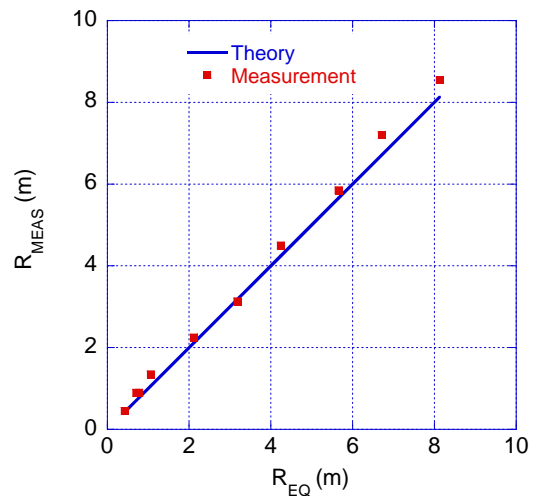


Fig. 6. Measured distance as a function of the equivalent obstacle distance.

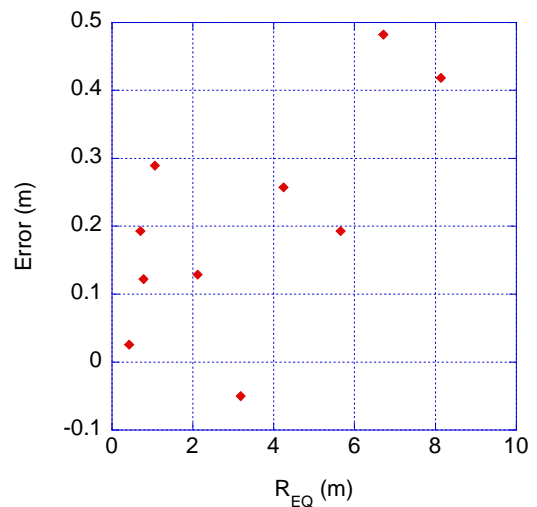


Fig. 7. Differences between measured obstacle distance and the equivalent obstacle distance as a function of the equivalent distance itself.

4. CONCLUSIONS

In this paper the design and test of a FMCW radar to be used as electronic travel aid for visually impaired subjects has been presented. The sensor is based on the Infineon BGT24MTR11 IC whose output frequency has been controlled by the Analog Devices AD4158 IC. Two serial arrays of patch antennas have been designed and realized. The designed sensor uncertainty has been experimentally investigated, finding a worst case value close to the theoretical resolution of 0.6 m calculated from the FMCW signal band. Future developments of the radar will be the integration of the two IC's and of the antennas on a single board. Moreover, particular attention will be devoted to the design of an ad hoc interface to communicate the obstacle distance information to the user. It is worth to be noted that, with respect to other similar ETA's located on belt or backpack, the proposed sensor utilizes the white cane that is very familiar for visually impaired subjects and hence is expected to be easily accepted.

ACKNOWLEDGMENTS

The Authors wish to thank Dr. Irene Babudri of Infineon Italy for providing the BGT24MTR11 integrated circuit.

REFERENCES

- [1] World Health Organization, "Visual impairment and blindness", <http://www.who.int/mediacentre/factsheets/fs282/en/>
- [2] C. Corcoran, G. Douglas, S. Pavey, A. Fielding, M. McLinden and S. McCall, "Network 1000: the changing needs and circumstances of visually-impaired people: project overview", *The British Journal of Visual Impairment*, vol. 22, No. 3, 2004, ISSN 0264-6196.
- [3] B.B. Blasch, W.R. Wiener, R.L. Welsh, *Foundations of Orientation and Mobility*, Second Edition, 1997.
- [4] U.R. Roentgen, G.J. Gelderblom, M. Soede, L.P. de Witte, "Inventory of electronic mobility aids for persons with visual impairments: a literature review", *Journal of Visual Impairment & Blindness*, vol. 102, no. 11 pp. 702-724 Nov. 2008.
- [5] D. Dakopoulos, N.G. Bourbakis, "Wearable obstacle avoidance electronic travel aids for blind: a survey", *IEEE Transactions on Systems, Man, and Cybernetics, Part C: Applications and Reviews*, vol.40, no.1, pp. 25-35, Jan. 2010.
- [6] National Research Council, "Electronic travel aids: new directions for research", Washington, DC: The National Academies Press, 1986.
- [7] L. Scalise, V. Mariani Primiani, P. Russo, D. Shahu, V. Di Mattia, A. De Leo, and G. Cerri, "Experimental investigation of electromagnetic obstacle detection for visually impaired users: a comparison with ultrasonic sensing", *IEEE Transactions Inst. Meas.*, vol. 61, no. 11, November 2012.
- [8] S. Linz, G. Vinci, S. Mann, et al., "A compact, versatile six-port radar module for industrial and medical applications", *Journal of Electrical and Computer Engineering*, vol. 2013, Article ID 382913, 10 pages, 2013.
- [9] P. Bernardi, R. Cicchetti, S. Pisa, E. Pittella, E. Piuze, O. Testa, "Design, realization, and test of a UWB radar sensor for breath activity monitoring", *IEEE Sensors Journal*, vol. 14, no. 2, pp. 584-596, Feb. 2014.
- [10] E. Pittella, P. Bernardi, M. Cavagnaro, S. Pisa, and E. Piuze, "Design of UWB antennas to monitor cardiac activity", *J. Appl. Comput. Electromagn. (ACES)*, vol. 26, no. 4, pp. 267-274, April 2011.
- [11] C. Frank, "Development and manufacturing of radar modules for automotive applications", *European Microwave Week*, 2013.
- [12] A.G. Stove, "Linear FMCW radar techniques", *Radar and Signal Processing, IEE Proceedings F*, vol. 139, no. 5, pp. 343-350, Oct. 1992.